2
Materials and Experimental Techniques

In this chapter, we will briefly discuss about the deposition and characterization techniques of different MO_x as well as other additive materials.

2.1 MATERIALS FOR MO_x BASED GAS SENSORS

2.1.1 TiO_2

Titanium dioxide (TiO_2) is n-type semiconductor with wide bandgap material [Wunderlich *et al.*, 2004]. It has excellent optical, electrical, photocatalysis, and gas sensing properties [Bai *et al.*, 2014]. Apart from this, it is nontoxic and low cost material. Normally, TiO_2 exists in three forms in nature, which is known as Anatase (tetragonal), rutile (tetragonal) and brookite (orthorhombic) as shown in Figure 2.1. Here, both anatase and brookite are metastable phases which are transformed into irreversible rutile phase at the temperature range around 400-800°C [Hu *et al.*, 2003]. Anatase and rutile phase of TiO_2 are mostly used in gas sensors. In both forms of TiO_2, each Ti atom is attached with six oxygen atoms in the crystal structure which creates a TiO_6 octahedron. However, both anatase and rutile are members of orthogonal crystal system but the distorted degree of each TiO_6 octahedron has few differences.

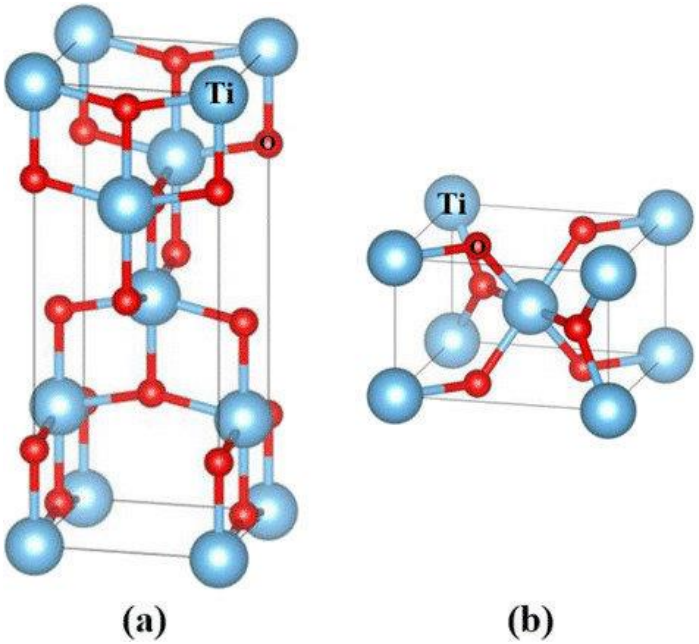

Figure 2.1: Crystal structure of (a) anatase (b) rutile (Source: *Jia et al.*, 2016)

2.1.2 ZnO

ZnO is known as II-VI semiconductor and has fascinating properties like high electron mobility, high chemical stability, broad range of radiation, good transparency, high photostability, low toxicity, biocompatibility and wide bandgap [Radzimska *et al.*, 2014]. Generally, ZnO has three types of crystal structures: hexagonal wurtzite, zincblende, and

rocksalt as depicted in Figure 2.2. Among these, hexagonal wurtzite crystal structure of ZnO is most stable and most common at ambient environment. The lattice constants of hexagonal wurtzite structure are found: a = 3.25 Å, and c = 5.2 Å, where the ratio of c/a ~ 1.60 which is approximately close to the ideal value of hexagonal cell (c/a = 1.633) [Ozgur *et al.,* 2010].

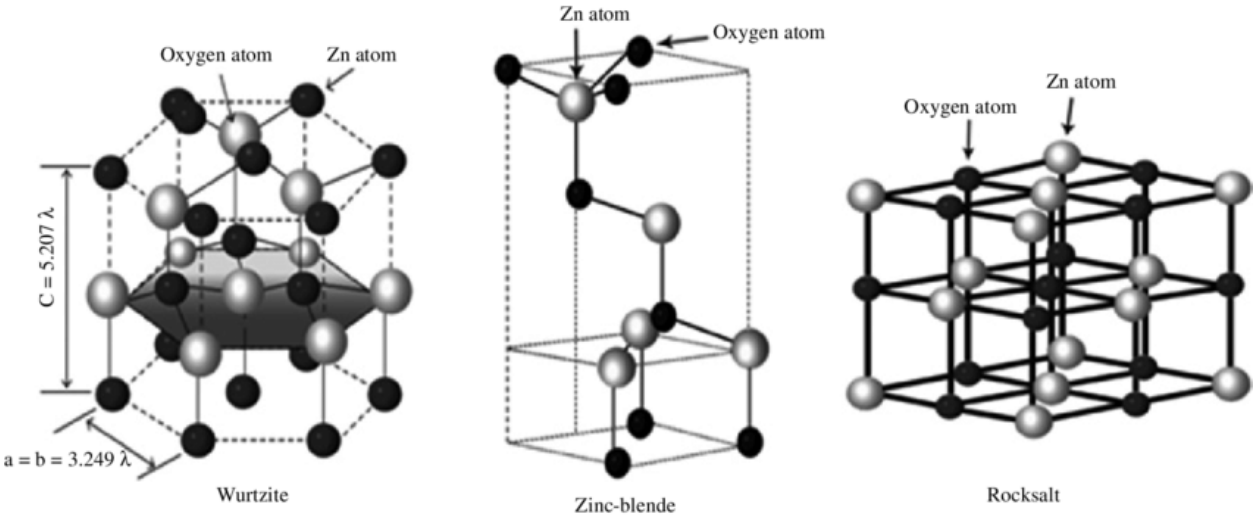

Figure 2.2: Different types of crystal structures of ZnO (Source: Özgür *et al.*, 2005)

ZnO has large direct bandgap (3.37 eV) and high exciton binding energy (60 meV) which makes it a potential candidate in the optoelectronics. In addition, it possesses good tolerance against high electric field, low electronic noise, high power operation, and higher breakdown voltages [Rai *et al.,* 2012; Zheng *et al.,* 2009]. Moreover, bond nature of ZnO is mostly ionic which makes it suitable for piezo and pyroelectric properties. These properties of ZnO are to applicable in energy generator, photocatalysis, sensors, and converter [Ranwa *et al.,* 2014].

2.1.3 V_2O_5

Vanadium oxides make a fascinating group of materials due to their different oxidation states from V^{2+} to V^{5+}. Till now, several types of vanadium oxides are reported such as VO, VO_2, V_2O_3, V_2O_5, and V_6O_{13} [Surnev *et al.,* 2003]. Amidst, vanadium pentaoxide, V_2O_5 has been attracted significantly because of broad applications. It exhibits superior properties like direct bandgap (2.3 eV), good thermal and chemical stability, and good thermoelectric properties. As the d^0 electronic configuration found in V^{5+} ions, which create active sites for incoming gas molecules and catalyze reactions. Generally, V_2O_5 is an n-type semiconductor oxide material and the conductivity of V_2O_5 increases when V^{5+} ions reduce to V^{4+} in the presence of reductive gases [Kofstad *et al.,* 1972]. V_2O_5 is widely used in several applications such as thermoelectric devices, electronic and optical switches, and solid state batteries [Le *et al.,* 2019]. Further, V_2O_5 acts as a heterogeneous catalyst, and this property is strongly related to the gas sensing application. Thus, we can add this material in the category of MO_x based gas sensor.

2.1.4 Reduced Graphene Oxide (rGO)

Graphene is a crystalline allotrope of carbon atoms, which has a single layer of carbon atoms in a 2-dimensional hexagonal structure [Geim *et al.,* 2007]. It is a zero bandgap semiconductor as both its conduction and valence bands touch at the Dirac points [Neto *et al.,* 2009]. Each atom of graphene has four bonds. The first one is σ bond which is formed due to the presence of its three neighboring carbon atoms, and second one is π-bond which is situated out of plane. Graphene has gained lot of attention in gas sensing applications over the last decades due to its excellent properties like high electron mobility, large surface-to-volume ratio, and good chemical stability [Chatterjee *et al.,* 2015]. Although, pristine form of graphene contains deficiencies of surface defect sites which display poor attachment of functional groups. These

functional groups are mainly responsible for enhanced gas-sensing properties. Therefore, a modified graphene (or reduced graphene oxide (rGO)), has become an eminent candidate as a gas sensors [Hu *et al.,* 2013].

2.1.5 Carbon Nanofibers (CNF)

1-D carbon nanofibers (CNFs) are very useful for gas sensors due to their superior qualities such as good chemical and thermal stability and high surface to volume ratio [Kim *et al.,* 2017]. There are several methods to synthesize the CNFs. Among them, electrospinning method is one of the most efficient ways because of ease of fabrication, cost-efficient, and simple techniques. These CNFs show directional morphology, and have excellent electrical characteristics as compared to carbon clusters. Moreover, nanoporous CNFs contain large surface area, excellent pore structure, and good surface reactivity which are essential properties for a gas sensor [Bai *et al.,* 2016]. Additionally, oxygenous functional groups are also attached on the surface of CNF. This results in increase in the gas reactions with functional groups, due to which sensitivity enhances. These surface defects or functional groups can be introduced via acid treatment.

2.1.6 Doping of Transition Metals Elements

Several studies have been performed for improvement of sensing response of MO_x based gas sensing via doping. Transition metal elements such as Co, Ni, Fe, and Cu have become more popular as dopants in MO_x [Zhang *et al.,* 2017; Maswanganye *et al.,* 2017; Bai *et al.,* 2014;Gong *et al.,* 2006]. These dopants not only increase the activation energy, but also change the resistance of the sensor. The main aim of these dopants is to reduce the operating temperature of MO_x, increase the sensing response, enhance selectivity, speed-up response, and provide stability towards the incoming gas molecules [Bhati *et al.,* 2018]. It has been seen that the particle size of MO_x reduces when a dopants is introduced in MO_x, which is caused by the restriction of particle growth during nucleation, since dopants stop further growth [Maciel *et al.,* 2003]. Apart from this, the surface morphology of MO_x also changes when the dopants are added in it. Smaller particle size have high surface area, which increases the large number of chemisorbed oxygen ions as well as barrier height, that leads to enhanced gas sensing response.

2.2 DEPOSITION TECHNIQUES

The deposition of thin films or other nanostructured materials of MO_x is the most fundamental step in all applications. Usually, an active layer is deposited onto the substrate material. There are two types of deposition techniques available for the growth of nanostructured materials: (a) physical vapor deposition techniques (PVD), and (b) chemical vapor deposition (PVD) techniques. In order to obtain the high quality thin films or nanorods like structure, PVD techniques have become very popular due to the benefits, such as good adhesion on substrate, excellent uniformity, and good stability over the periods. Thus, PVD technique has great usage in many applications such as gas sensors, optoelectronics and photodetectors. For this purpose, the deposition of 1-D nanostructures and thin films is highly essential. Once the active layer of MO_x has been established on the desired substrate, the fabrication of metal contacts on active layer as well as substrate needs to be properly performed. Such requirement can be accomplished using thermal evaporator system or lithography techniques. The adhesion of the metal contact should be excellent, which is needed for electrical characterization and gas sensing measurement. However, the decoration of nanomaterial on the MO_x using drop casting is also a facile technique. Therefore, RF sputtering techniques and drop casting method is discussed for MO_x deposition and decoration of nanomaterial, respectively. Then, thermal evaporation techniques and lithography will be briefly explained for the fabrication of metal contacts.

2.2.1 RF Sputtering

Among all PVD techniques, radio frequency (RF) sputtering is a very important technique for the growth of semiconductor and insulator. Mass production for thin film coating

of metal as well as semiconductor has become possible using RF sputtering. Some excellent features make this technique very popular such as good adhesion thin film on substrate, growth at low temperature, low cost, and continuous substrate rotation. Sputtering is a process, in which a material is attacked by high energy ions, so that the surface of material obtains sufficient energy to further extract the atoms from target material; and these extracted atoms freely move towards the substrate. The whole process of sputtering deposition takes place in high vacuum chamber. Sputtering target is mounted on the RF magnetron, which acts as a cathode. On the other hand, substrate is fixed on the substrate holder which works as an anode. The substrate can be heated at high temperature during the deposition process. Substrate holder is mounted on the heater to provide uniform substrate heating. In order to minimize the contamination level, the sputtering chamber needs to be highly evacuated (~10^{-6} mbar). Such type of vacuum level increases the mean free path of the extracted atoms which has to be deposited on the substrate. High vacuum can be achieved inside the chamber using rotary pump followed by turbo pump. Argon (Ar) gas and other reactive gases (like N_2 and O_2) are injected into sputtering chamber with high accuracy using mass flow controller (MFC). RF power, substrate temperature, target to substrate distance, chamber pressure, and gas flow rates are the main factors for the sputtering deposition process, and the quality of thin films and other nanostructures which can be modulated by changing these parameters.

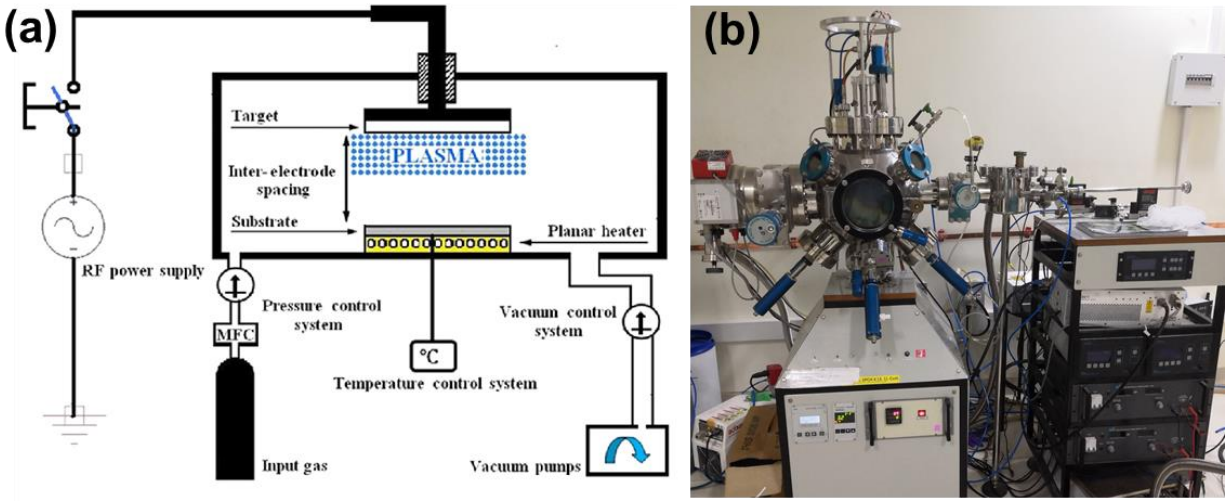

Figure 2.3: (a) Schematic diagram of sputtering process (Source: Yasrebi *et al.*, 2014) (b) Experimental setup of RF sputtering system at IIT Jodhpur

Figure 2.3 (a) shows the basic diagram of RF magnetron sputtering system. Once high vacuum level is achieved, highly pure Ar gas is injected into the sputtering chamber at constant flow rate due to which working pressure is maintained in the sputtering chamber. When constant RF power is applied between the substrate and target material, an electric field is created between them. Initially, target material is negatively biased (target is placed on the RF magnetron) and substrate is positive biased. i.e. high energy electrons are extracted from the target material that accelerate towards the substrate. Then, these electrons will interact with argon gas and ionize it as Ar^+ ion. During this interaction, secondary electrons are also produced which further interact with argon gas, leading to creation of large number of Ar^+ ions. Thus, formation of dense plasma occurs inside the chamber and atoms are ejected from the target material. These ejected atoms are then deposited on the substrate. However, the sputtering yield strongly depends on the growth parameter. In order to make oxide and nitride thin film, reactive gases like oxygen, and nitrogen, respectively can be used. Figure 2.3 (b) illustrates the complete setup of RF magnetron sputtering system (Excel Instruments).

2.2.2 Photolithography

Photolithography is a process of transferring the pattern on the surface of substrate using mask. This process requires three major parts which are UV source, photo mask, and photoresist. The photolithography involves some basic steps such as wafer cleaning, deposition of MO_x layer or SiO_2 layer, coating of photoresist, soft baking, mask alignment, UV exposure, development, and hard baking [Sheats, 2007]. Photoresist is known as photosensitive material which has two types: positive and negative. Positive photoresist is more soluble, while negative is less soluble after exposure to UV light. Firstly, the photoresist material is adhered on the substrate. After that, the sample surface is exposed to UV rays that change the molecular structure of the photoresist material followed by modification of its solubility, while keeping the mask of pattern intact. Thereafter, etching process is carried out, where the substrate undergoes through the developer solution. The main aim of the developer is to dissolve the exposed region of the photoresist coated substrate during UV exposure. Figure 2.4 depicts the mask aligner for photolithography which is available at IIT Jodhpur.

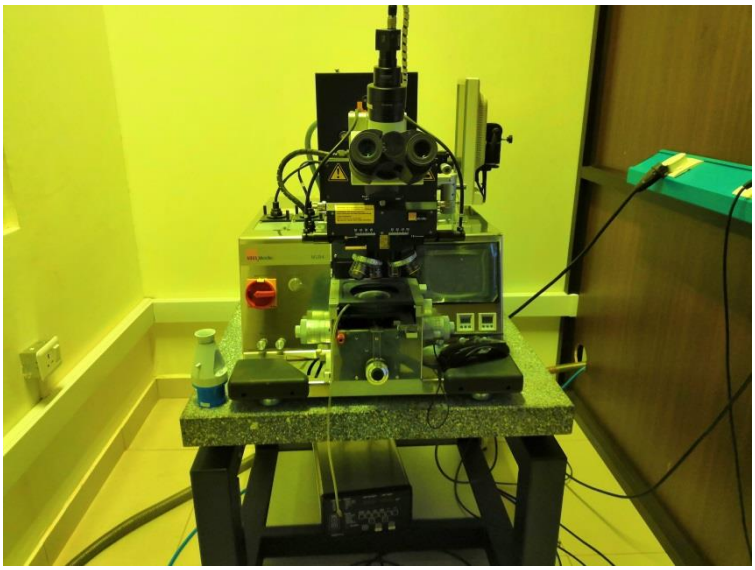

Figure 2.4: Mask Aligner setup for photolithography at IIT Jodhpur

There are also some other lithographic techniques such as electron beam lithography and X-ray lithography which gives better resolution.

2.2.3 Drop Casting

Drop casting method is one of the simplest and cost effective approaches among other techniques. This method involves placing drops of the solvent containing the applicable material on the substrate followed by evaporation of the solvent by heating. It is wet chemical method which usually produces thin layer of materials. However, thickness of the material depends upon the total number of drops to be deposited on the substrate. It should be noted that interaction between the solvent containing materials and surface of substrate must be larger than the intermolecular interaction, leading to elimination of the problem of cluster formation during deposition on the substrate. In this Thesis, rGO particles and carbon nanofibers (CNFs) containing solvents were used. Drop casting is done between the fingers of the interdigitated electrodes (IDE) pattern MO_x nanostructures (mostly ZnO) with subsequent heating upto 100˚C to evaporate the solvents completely. Finally, we have made p-n heterojunction between p-type rGO/CNF and n-type ZnO. Figure 2.5 shows the basic fabrication steps in drop casting method which are employed to fabricate decorated nanoparticles on MO_x nanostructures.

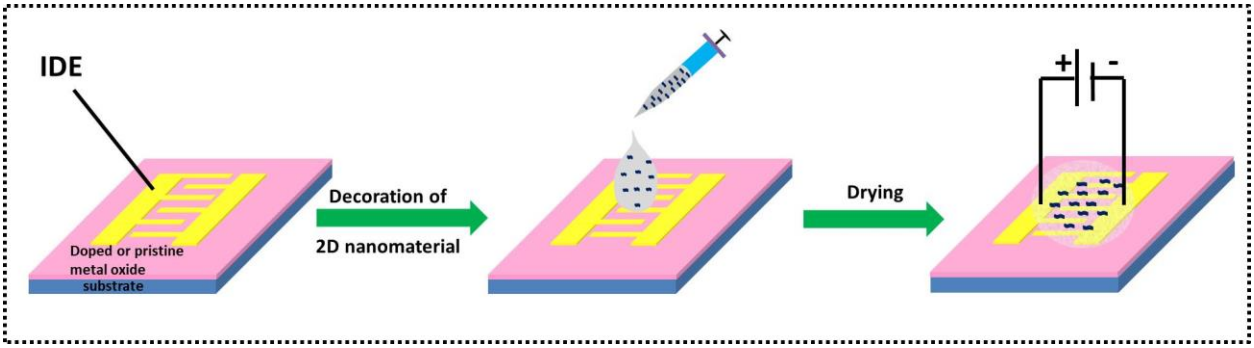

Figure 2.5: Schematic diagram of fabrication steps in the drop cast method

2.2.4 Thermal Evaporation

This technique is broadly used for fabricating metal electrodes on the surface of the substrate. However, the deposition of non-metals such as oxides and nitrides are also possible using this technique. The thickness of deposited material can be altered as per the need of many applications which depends on deposition time and evaporation rate. The deposition of metal electrodes occurs using the shadow mask with different pattern, which should be fixed on the top of the substrate. Moreover, different layers of thin film can be generated on the substrate by using thermal evaporation. A high level of vacuum environment is required to minimize contamination. Thus, it requires at least 10^{-6} mbar to start the deposition process of the thin film. A high vacuum pump such as, diffusion pump/turbo pump along with rotary pump is required to achieve vacuum. Once vacuum is created inside the chamber, the source material is heated above its melting point, due to which the material gets evaporated.

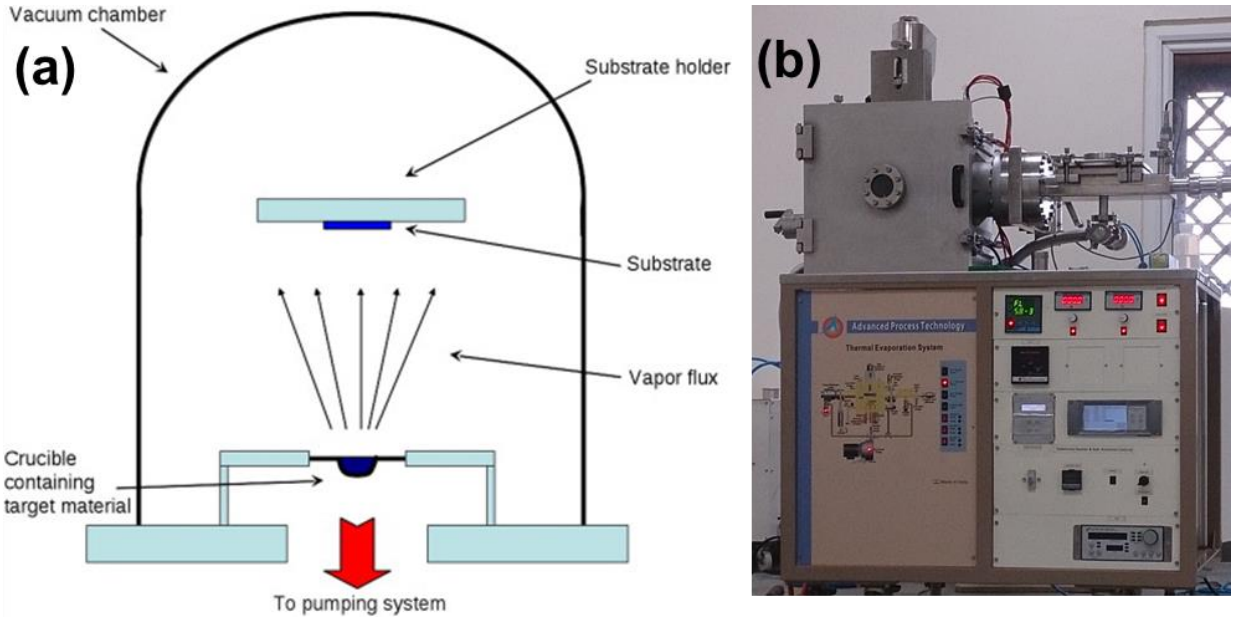

Figure 2.6: (a) Basic diagram of thermal evaporation (Source: Lakhtakia *et al.*, 2013) (b) Thermal evaporation system at IIT Jodhpur

Finally, the evaporated material settles down onto the substrate material which is placed just above the target, thus leading to formation of thin film. As the substrate has lower temperature as compared to target material, the evaporated molecules give energy to the substrate, and deposit as a thin film due to the condensation process. The source material is placed either in resistive heating filaments or metal boats (Mo/W is used). These metal boats/filaments can sustain high temperature. When a constant voltage and high current is applied to these metal boat/filaments, the source material is evaporated above its melting point,

which finally settles down on the substrate material. This technique provides a uniform step coverage and adhesion on the substrate. The thickness of the deposited material can be calculated using quart crystal microbalance during the deposition process which gives a rough value. Figure 2.6 (a) and (b) represents the basic diagram of thermal evaporation, and experimental setup of thermal evaporation system, respectively.

2.3 CHARACTERIZATION TECHNIQUES

2.3.1 X-Ray Diffraction (XRD)

XRD is one of the most important techniques in material science and mainly used to obtain the information of crystal structure. This technique can give some fascinating information such as grain size, chemical composition, orientation of plane, and stress/strain studies [Cullity, 1978]. It is well known that the atoms are arranged in regular manner in their unit cell which makes the structures of materials crystalline. The basic working principle of XRD relies on the constructive interference.

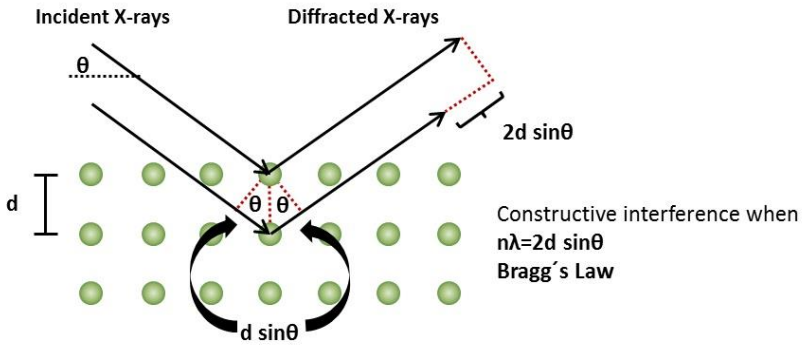

Figure 2.7: Schematic diagram of Bragg's Law (Source: https://wiki.anton-paar.com/en/x-ray-diffraction-xrd/)

When a monochromatic X-ray is interacted with the target material, the X-ray beam gets scattered through the atoms of target material (atoms are arranged in crystalline plane) that form a diffraction pattern due to constructive inference of detected X-rays. These incident X-rays are generated by cathode ray tube (CRT) using a radiation source (Cu-K) whose wavelength is 1.54 Å. Interestingly, the generation of monochromatic X-ray beams is achieved by filters. Therefore, these beams are passed through the collimator in order to properly align towards the direction of sample holder. Once the X-ray beams interact with the sample, it gets diffracted and collected by the detector. During the X-ray scanning of the samples, the possibility of scanning becomes high for all the possible crystallographic planes of material due to scanning at 2θ diffraction angle. In order to get the X-ray peak for specific orientation of the crystal structure, Bragg's law must be obeyed due to constructive interference; as shown in Figure 2.7. If X-rays are incident on the material at θ angle and then diffracted from the crystallographic plane having d interatomic distance, then Bragg's law will be according to Eq. (2.1) [Hammond, 2001]:

$$n\lambda = 2dsin\theta \tag{2.1}$$

where λ is X-ray wavelength (1.54 Å for Cu-K_α) and n represents an integer. Figure 2.8 displays the XRD system (D8 Advance Bruker) available at IIT Jodhpur.

The analysis of peak broadening of XRD spectra will give rise to the crystallite size of the particle. Normally, peaks in XRD patterns are not always sharp. They rarely come out to be broad. This may be due to instrumental factors or the presence of small crystalline size (nanoparticles).

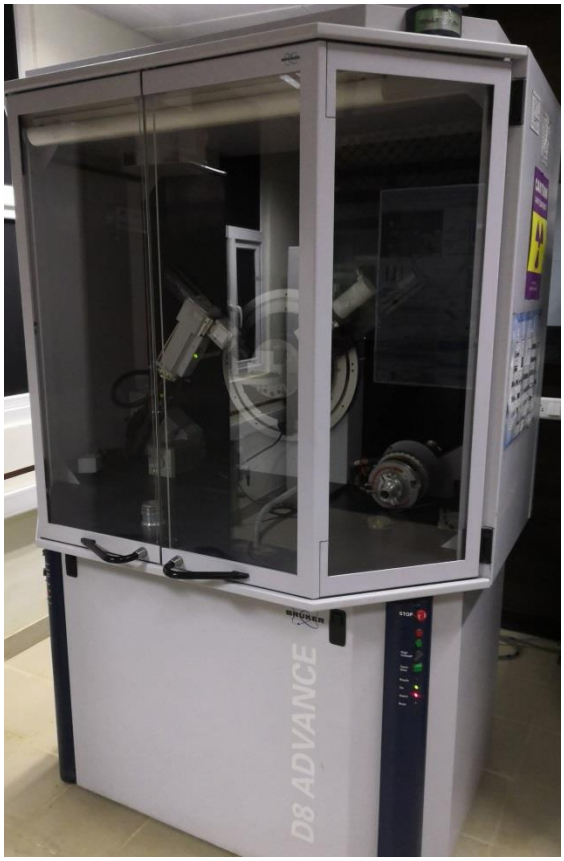

Figure 2.8: Powder XRD machine at IIT Jodhpur

The peak broadening increases as the size of crystallite decreases and can be calculated using Scherrer's equation as shown in Eq. (2.2):

$$\beta = \frac{K\lambda}{Dcos\theta} \tag{2.2}$$

where K is Scherrer constant, λ is wavelength of radiation, D is crystalline size, θ is Bragg angle, and β is full width half maximum (FWHM) of a peak in XRD pattern. Moreover, the peak broadening in nanocrystalline materials will also lead to the microstrain. This occurs due to lattice strain created by the dislocation of unit cell from their normal position. Sometime it is also caused by the dislocation of grain boundaries, where the microstrain can be seen according to the below Eq. (2.3).

$$\beta = 4\varepsilon\frac{sin\theta}{cos\theta} \tag{2.3}$$

Here, ε is microstrain present in the nanocrystalline material.

2.3.2 Field Emission Scanning Electron Microscopy (FESEM)

FESEM is an instrument which provides wide information like surface morphology, distribution of nano/microstructure, surface image with high resolution, and thickness of the deposited material. A basic diagram of FESEM is shown in Figure 2.9 (a). In the working principle of FESEM, a highly focused electron beam scans the sample surface which produce high resolution surface image. First of all, electron beams are emitted from electron gun (field emitters as cathode) and then passed through the anode. The accelerating voltage between cathode and anode is usually set in the range of 0.2-20 KV. In the entire operation, a high vacuum environment (~10^{-6} mbar) is required in the FESEM chamber. In order to focus the primary electron beams more precisely, an electromagnetic lens is used, which then deflects the electron beam. The electron beam diameter must be smaller than the feature size which gives high resolution surface image. When a primary electron beam is interacting with the sample

surface, then secondary electrons are ejected from the sample surface and collected by the secondary detector. This will produce the surface topography of the desired sample. Moreover, different emission angles of secondary electrons and their velocity provides information related to surface structure at different locations. Except secondary electrons, other information such as backscattered electrons, X-rays, Auger electrons, and cathadoluminescence can be obtained from the sample surface (upto depth ~5 μm) (Figure 2.10).

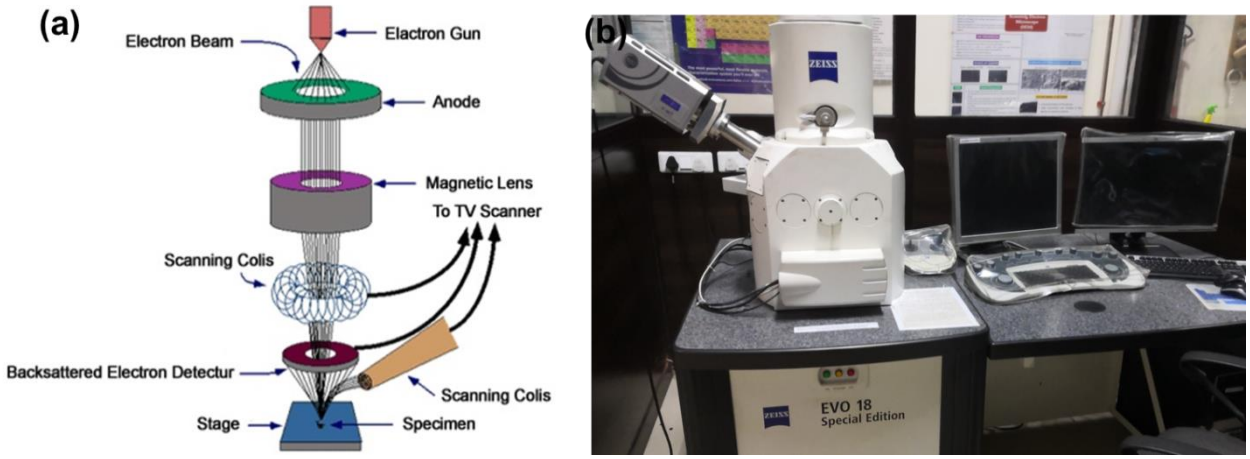

Figure2.9: (a) Schematic diagram of scanning electron microscopy (Source: https://sites.google.com/site/frontierlab2011/scannig-electron-microscope/principie-of-sem) (b) SEM facility available at IIT Jodhpur

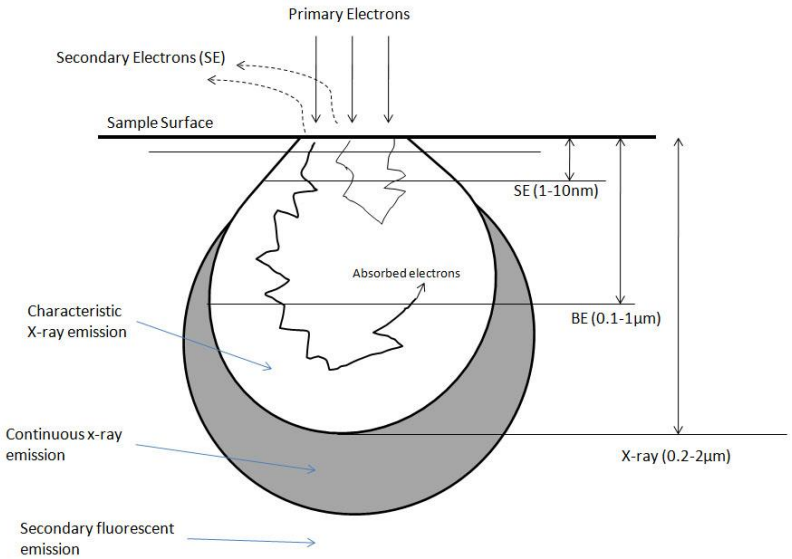

Figure 2.10: Schematic diagram of various information generated from the sample (upto depth ~ 5μm) during interaction of primary electron (Source: https://chem.libretexts.org/Bookshelves/Analytical_Chemistry/Book%3A_Physical_Methods_in_Chemistry_and_Nano_Science_(Barron)/09%3A_Surface_Morphology_and_Structure/9.3%3A_SEM_and_its_Applications_for_Polymer_Science)

Generally, an X-ray Dispersive Energy Detector (EDX or EDS) is also attached with the FESEM equipment which is used to study the elemental analysis. FESEM is similar to SEM but it gives far better surface resolution and higher energy range than SEM. Apart from this, the working principle of FESEM is same as that of SEM, the only difference being their electron

generation system. The generation of electrons in SEM is processed using heated tungsten filament (thermal emission source). However, in the case of FESEM, a field emission gun is used which provides highly focused electron beams with different energy ranges. Therefore, the spatial resolution of the sample surface improves at low operating voltage (0.02-5 KV). Consequently, the charging effects can be minimized on the non-conductive samples, which also prevents the electron beam's sensitive sample surface. Here, experimental set up of SEM used in IIT Jodhpur can be seen in Figure 2.9 (b).

2.3.3 Atomic Force Microscopy (AFM)

AFM is the characterization technique which is used to provide surface morphology with less preparation of sample, and high resolution of surface image with three dimensions. A sharp tip (Si or Si_3N_4) with few nm of diameter is mounted on the hanging end of the cantilever. A basic diagram of AFM is shown in Figure 2.11 (a). When an AFM tip gets closer to the sample, the cantilever is deflected because of force generated between the tip and the sample surface. Therefore, AFM calculates these forces with regard to van der walls forces or mechanical forces. AFM detects these forces in either non-contact or contact mode which depends upon the tip and sample surface. AFM tip having frequency of 100-400 KHz vibrates over the sample surface with small amplitude in non-contact mode. Most interestingly, distance between the tip and the sample is maintained to few angstroms during scanning. When tip is much close to the sample surface, a repulsive force increases on the cantilever. However, when the distance between the tip and the sample becomes sufficiently higher, attractive force remains between the tip and the sample in van der wall force range. This will lead to the deflection on cantilever, which occurs either on the sample side or away from the sample depending on the surface features. Apart from this, a laser beam is closely focused on the position of the cantilever, and a photo detector is used to capture the deflected beam. The deflection of laser beam is due to the moderation of cantilever position which is caused by the variation of surface morphology. Photo detector takes signal from the deflected beam in the z-direction at each X-Y location of the sample during scanning, and converts it to electrical signal.

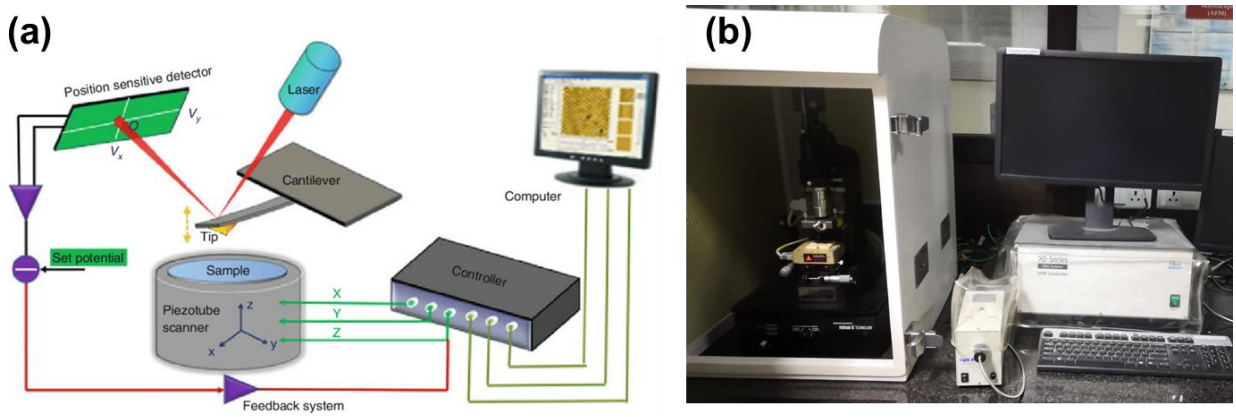

Figure 2.11: (a) Basic diagram of the working principle of AFM (Source: Guo *et al.*, 2013) (b) Experimental set up of AFM facility at IIT Jodhpur

Therefore, surface topography images of the sample are constructed once the signal passes through the feedback electronics and is realized from the AFM scanning software. Another use of AFM is to find out surface roughness and line profile of the morphology in the given area. Figure 2.11 (b) represents the AFM instrument available at IIT Jodhpur (Park XE-70).

2.3.4 Ultraviolet-Visible (UV) Spectroscopy

UV spectroscopy is used to measure the absorption of light by a material in the UV spectral region. This means that the technique utilize light in the visible or nearest ranges like near-UV and near infrared range (NIR). The absorption of UV light leads to the excitation of

electrons to higher energy level. The energy of absorbed UV light is equal to the energy difference between the lower energy states to higher energy states. This instrument is used to perform a quantitative analysis of the absorber concentration in the solution of transition metal ions as well as conjugated organic molecules. The basic working principle of a UV spectrometer is based on the Beer-Lambert law. When a monochromatic laser beam is passed through the solution of absorbing material, the rate of decreased light intensity depends upon the thickness of the solution, and is proportional to the incident laser light.

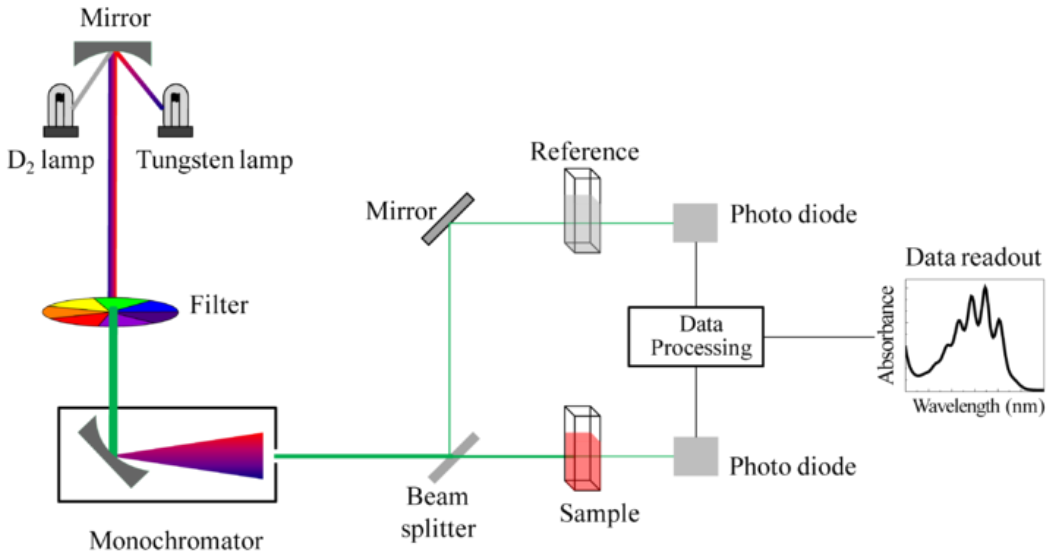

Figure 2.12: Basic diagram of UV visible spectrophotometer (Source:https://commons.wikimedia.org/wiki/File:Schematic_of_UV_visible_spectrophotometer.png)

The main components in UV spectroscopy are light source, monochromator, reference and sample cells, detector, and amplifier. Figure 2.12 shows the basic diagram of UV visible spectrophotometer. The determination of band gap of MO_x material is possible using UV spectrometer. The Taue method is used to measure the band gap by plotting a graph between $(\alpha h\upsilon)^{1/n}$ and energy of photon ($h\upsilon$), where α is the absorption coefficient that can be computed from absorbance (A). The thickness of the sample (t) can be realized as ($\alpha = 2.3A/t$) and photon energy can be calculated by using $h\upsilon = 1240/\lambda$. Moreover, the values of power factor (n) can be taken as 0.5 and 2 for direct and indirect transitions, respectively. Finally, the extrapolation of straight line through the curves on $h\upsilon$ (X-axis) will provide a band gap of MO_x.

2.3.5 Raman Spectroscopy

Raman spectroscopy is a non-destructive characterization technique which gives information about phase, intrinsic defects, crystallinity, and chemical structure of the material. The basic working principle of this technique is based upon the light interaction with the bonds within a sample. It is a light scattering technique. When high intensity laser light is incident of the sample, the vibrating molecules within the sample scatter the incident laser light. This leads to formation of vibration modes in the form of different peaks depending upon the intensity as well as wavelength position in Raman Spectra. Each peak shows specific features in terms of molecular vibrations in bond such as C=C, C-H, and C-C etc. Since Raman spectra are a specific chemical fingerprint for the particular molecule or sample, it can be used to identify the sample quickly. Figure 2.13 shows the block diagram of Raman spectrometer. In the instrumentation of this technique, there is a laser light (visible, IR, and near IR) which is focused on the material using mirror assembly.

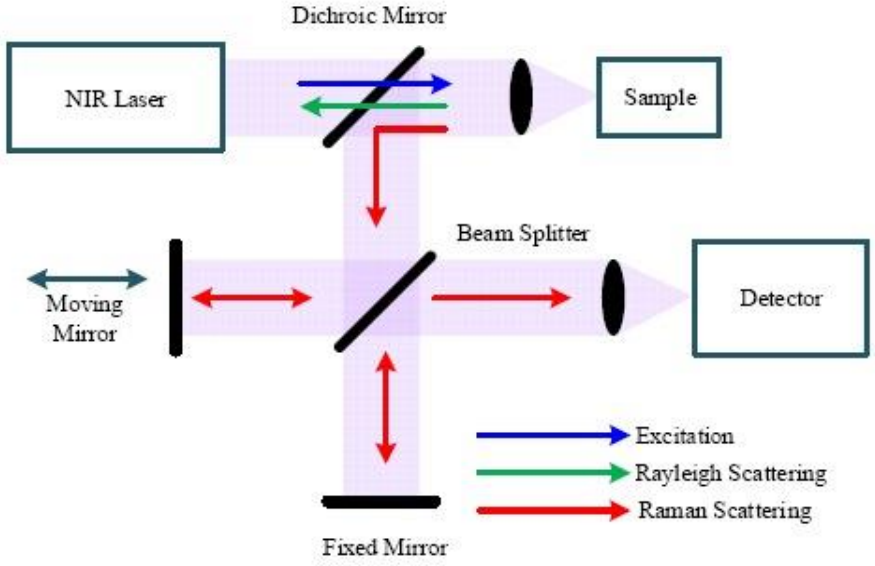

Figure 2.13: Block diagram of Raman spectrometer (Source: Li *et al.*, 2014)

Thereafter, the scattered light goes through the focusing lenses and notch filter; which are then collected by the spectrometer.

2.3.6 X-Ray Photoelectron Spectroscopy (XPS)

XPS is a useful technique in material science which is used to do elemental analysis. Generally, XPS identifies the elemental composition, oxidation state, and chemical shift of a particular element present in the sample [Reinert *et al.*, 2005]. In this technique, X-ray photon is interacted with the core electrons of the sample, resulting in the excitation of an electron from the atom and thereafter, removal from the sample. This ejected core level of electrons is also known as photoelectron. These core electrons have unique feature because its ejection from the core level of the particular atom also has different binding energy. Basically, there are three main tools which are used to measure these electrons: X-ray source (Al-K_α or Mg-K_α), sample, and e^- detector. The schematic illustration of photoemission process is shown in Figure 2.14. The entire process of the detection of electrons is carried out in high vacuum chamber which increases the mean free path of the electrons. Let suppose an X-ray photon having energy $h\mu$ is incident on the surface of the sample, and is absorbed by an atom whose binding energy is E_B. If $h\mu > E_B$, then electrons will be ejected from the sample with kinetic energy E_k. Therefore, these ejected electrons will be detected by the analyzer. So, binding energy of the electrons can be computed according to the below Eq. (2.4).

$$E_B = h\mu - E_k - \phi \qquad (2.4)$$

where, ϕ is the workfunction of electron.

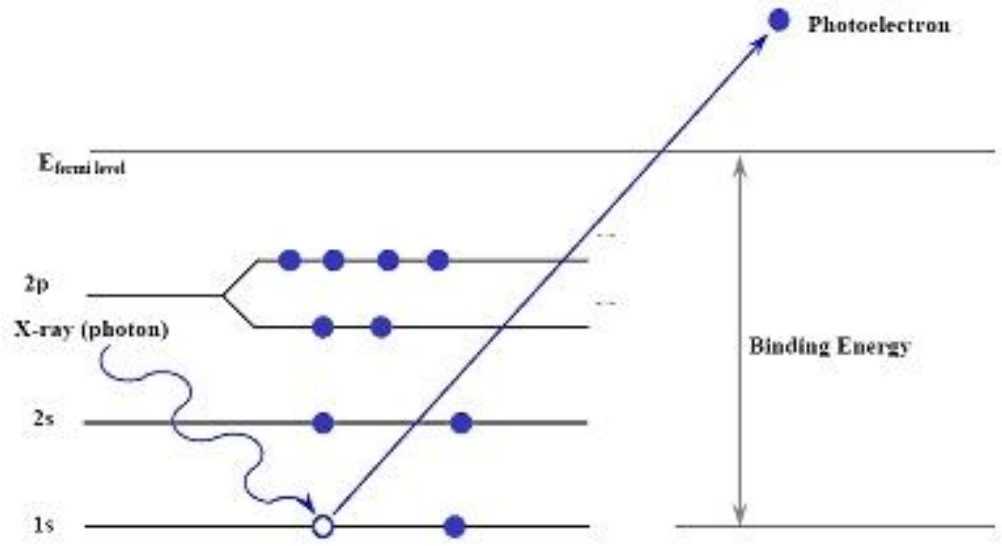

Figure: 2.14: Schematic illustration of photoemission process (Source: http://www.coretechint.com/technical_info-xps.php)

The detected electron gives useful information of different atomic species just near the sample surface (usually ~ 10 nm depth of film). Moreover, a slight shift in the binding energy is also useful, which is known as chemical shift. In XPS spectra, different peaks can arise at different binding energy which comes out from different core state of the sample surface. Thus, oxidation state as well as chemical shift of the chemical species at particular binding energy can be measured using the XPS spectra.

An ejected photoelectrons from depth d having initial intensity and intensity at which the electrons knock out from surface as I_0 and I_S, respectively. This effect can be described using Beer-Lambert is shown in Eq. (2.5).

$$I_S = I_0 e^{\frac{-d}{\lambda}} \tag{2.5}$$

In the above equation, λ shows inelastic mean free path of an electron. The thickness, at which 95% of photoelectrons are scattered while coming out to the surface, is usually achieved at a depth of ~3λ, which is known as sampling depth. The value of λ is around 1-3 nm for Al-K_α radiation that provides a sampling depth of 3-10 nm. For different oxidation states, the binding energy of electrons is different in the element. The binding electron of the core electrons is usually lower for the neutral atom as compared to the ion. The core level spectra of the XPS pattern is caused by the presence of spin-orbit coupling which leads to doublet states. Thus, useful information like, different oxidation states can be observed from multivalent cation in particular elements. Each surface atom has core electrons having specific binding energy, whose core level shift provides details regarding chemical bonding and valence states present in the thin film. Moreover, the valence band maxima (VBM) of the XPS spectra can be computed by drawing a tangent of valence band emission.

2.3.7 Fourier Transform Infrared Spectroscopy (FTIR)

FTIR is a useful technique used to investigate inorganic and organic materials. This method computes the absorption of infrared waves by the sample as a function of wavelength. The peaks corresponding to IR spectra tell about the molecular structure and its component. When IR radiation is interacted with the sample, few radiations are absorbed from the sample, and the remaining signal is transmitted. Absorption of IR by a sample leads to excitation of the molecule into higher vibrational energy state. The wavelength of light which is absorbed by molecules is closely related to the energy difference between the ground state and the excited

vibrational state. The wavelength, at which the molecules absorb the IR radiation, is a characteristic of the material.

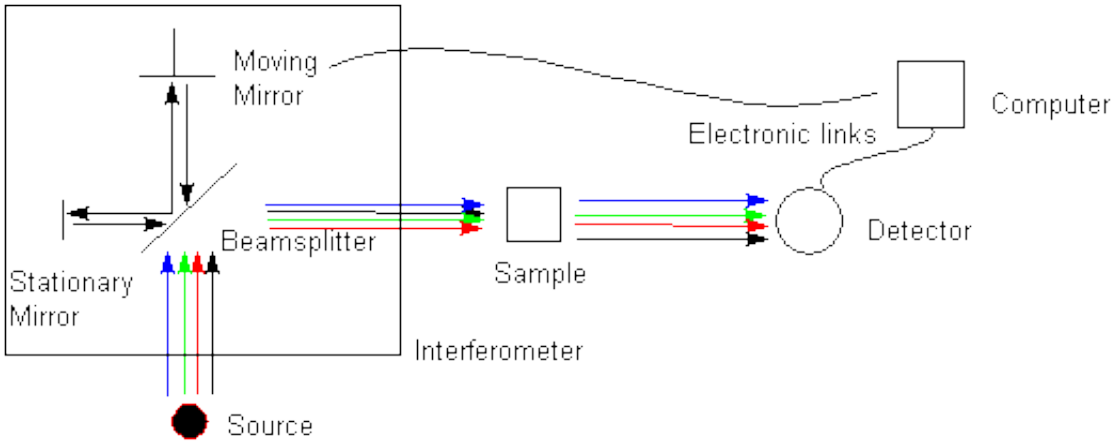

Figure 2.15: Schematic diagram of basic instrumentation of FTIR spectrometer (https://chemistry.oregonstate.edu/courses/ch361-464/ch362/irinstrs.htm)

An interferometer of FTIR is modulating the wavelength from IR source. While a detector measures the intensity of reflected as well as transmitted signal as a function of wavelength, the signal is converted using Fourier transforms. Thus, the final signal is represented as the percentage of intensity of light absorbed or transmitted versus wavenumber (cm^{-1}). In order to identify a material, the unknown IR spectra match with the known IR spectra of a material from the computer database. Therefore, the peaks originated on the IR spectra at different wavenumbers tell about the absorption band in the range 700-4000 cm^{-1} for functional groups such as C=O, -OH, and N-H. Figure 2.15 represents the basic instrumentation of FTIR spectrometer.

2.3.8 Kelvin Probe force Microscopy (KPFM)

KPFM is a non-contact and non-destructive technique which is used to measure the work function of a material. It is similar to AFM; however KPFM measures the contact potential difference (CPD) between the tip and the sample. The CPD can be transformed into work function of the sample at the equilibrium condition [Melitz *et al.*, 2011]. In KPFM, all the operation is conducted in the non-contact mode. Here, a conductive tip is oscillated on the sample surface at its first resonance frequency. Then the topographic data is extracted by adjusting the atomic force between the tip and the sample position. Moreover, a long range electrostatic force also acts between the tip and the sample, which is subsequently calculated by CPD between them. When an AC voltage is applied to the tip, an electrostatic force can be detected using lock-in amplifier. This AC voltage is fixed to the second resonance frequency of the cantilever. The electrostatic force becomes zero due to compensation of CPD when a DC voltage is applied to the tip. Thus, this CPD is equal to applied DC voltage which is also known as Kelvin voltage.

2.3.9 Electrical Characterization

Electrical characterization of materials is used to measure the carrier concentration, resistivity, contact resistance, barrier height, ideality factor, depletion width, impurity levels, and mobility. In this Thesis, we have measured the current-voltage (*I-V)* relationship of MO_x to find out the properties which may be Ohmic or Schottky junction. Also, the possibility of p-n heterojunction between n-type material and p-type material has been observed using I-V characterization. The two probe system has been used to investigate the electrical properties of Ohmic as well as Schottky junction in this characterization. Firstly, two probes were fixed on the

metal contact on the *I-V* characterization system, and the output of the probes was associated with source meter (Keitheley-4200 SCS).

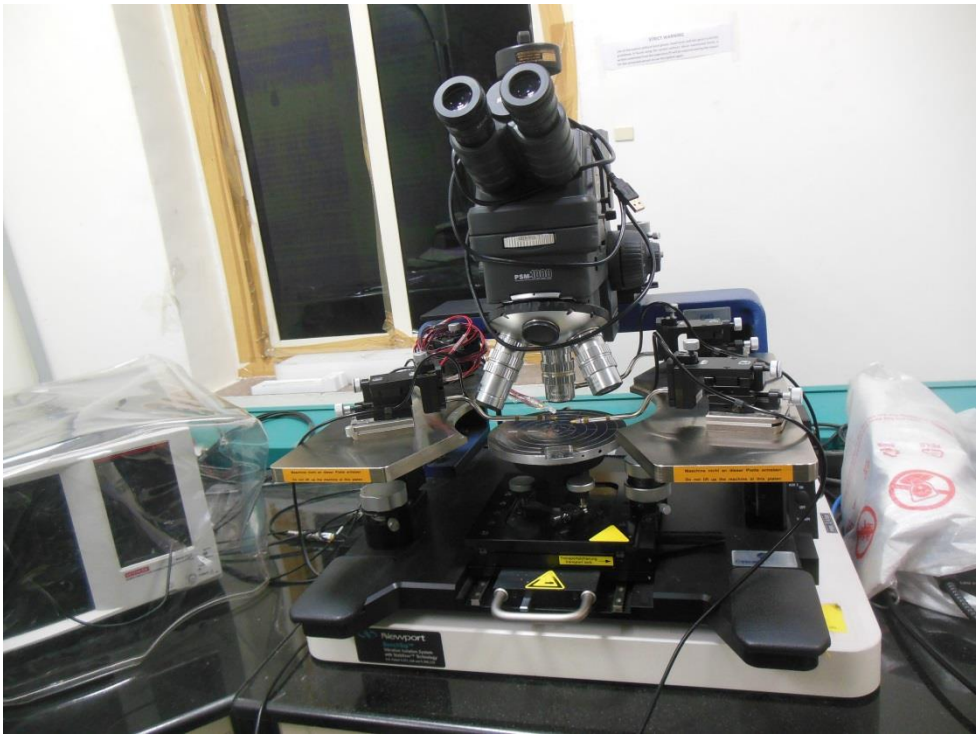

Figure 2.16: Experimental set up for electrical measurement at IIT Jodhpur

This source meter measures the heterojunction properties when constant voltage is applied and its corresponding current is changed. During the measurement, +3 to -3V voltage was applied in forward and reverse bias to check the electrical properties of the device. Figure 3.16 depicts the experimental set up for *I-V* characterization at IIT Jodhpur.

2.3.10 Gas Sensing Measurement

In order to obtain the gas sensor's characteristics, we have utilized a gas sensing chamber set up; which is optimized for different gases. A custom made stainless steel gas sensing chamber with gas inlet-outlet port is used. The main reason for using this closed sensing chamber is to provide isolation from external environment during exposure of hazardous and toxic gases. Figure 2.17 depicts the custom made gas sensing set up at IIT Jodhpur. First of all, gas sensing chamber was evacuated up to ~1×10^{-2} mbar with the help of rotary pump to avoid external effects during gas sensing. High operating temperature can be applied to the sensor using a heater. This heater is connected to the external DC supply on the gas sensing platform where temperature can be controlled using the variac. During gas sensing measurement, operating temperature of up to 150°C was given to the sensor. A thermocouple is also attached on the sensing platform which monitors the temperature regularly during the measurement. The main aim is to apply moderate temperature to the sensor to verify the ability of the sensor to work at low power. For gas sensing test, different type of gas cylinders (1% and 5%) are connected with the inlet port of the sensing chamber.

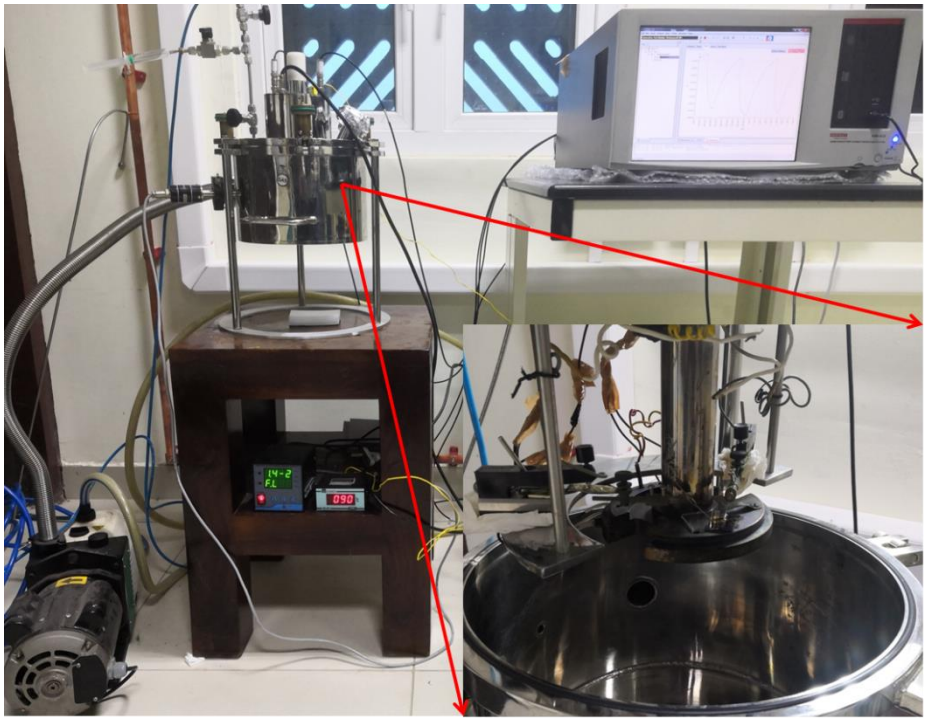

Figure 2.17: Customized gas sensing chamber used in IIT Jodhpur (Inset Figure shows the sample platform inside the gas chamber

When a sensor's baseline becomes constant on the computer screen, a known amount of gas is taken in gas tight syringe which is also connected with the inlet port of sensing chamber. The gas is then inserted in the sensing chamber. Therefore, change in base line occurs. Once the gas sensing response is saturated, one can open the outlet port of the sensing chamber, and can analyze the gas sensing response curve. Sensor characteristics such as sensing response, response time, and recovery time can be studied using the obtained curve. The calculation of target gas concentration can be done using Eq. (2.6) as

$$ppm\ (x) = \frac{volume\ of\ syringe\ (ml)}{volume\ of\ gas\ chamber\ (ml)} \times gas\ conc.\ in\ cylinder\ (ppm) \quad (2.6)$$

During the measurement, we have taken different gases like, oxidative and reductive gases to observe their sensing response for a particular gas sensing material.